

Machine Learning-Assisted Optimization of RF Power Amplifiers for High-Efficiency Wireless Transmitters

S. Praveen Kumar*

Assistant Professor, Department of Computer Science and Engineering, Mahendra Engineering College, Mallasamudaram, Namakkal district.

KEYWORDS:

RF power amplifier,
Machine learning,
Bayesian optimization,
Artificial neural network (ANN),
Power-added efficiency (PAE),
Surrogate modeling,
Harmonic balance simulation,
CMOS RF circuits,
Wireless transmitters,
Multi-objective optimization.

ARTICLE HISTORY:

Submitted : 19.09.2025
Revised : 14.11.2025
Accepted : 20.12.2025

<https://doi.org/10.17051/NJRFCS/02.03.03>

ABSTRACT

The power consumption of power amplifiers (PAs) dominates the modern wireless transmitters and thus there is a strong desire to improve efficiency as a design goal. But, high power-added efficiency (PAE) and gain and linearity are difficult to meet in RF design spaces, where the spaces are strongly nonlinear and non-dimensional. Traditional methods, e.g. load-pull analysis and tedious parametric sweeps, are computationally intensive and may be inefficient in multi-parameter optimization. The proposal in this paper is a machine learning-aided optimization of a 2.4 GHz Class-AB RF power amplifier that was designed in 65 nm CMOS technology. An artificial neural network (ANN) surrogate model which is trained with harmonic-balance simulation data will provide a high accuracy prediction of important performance quantities of a circuit, such as PAE, gain, and output power. Optimal bias voltages and matching network component values are then found with a performance constraint using Bayesian optimization. The suggested framework reaches up to 10.8% enhancement in PAE in contrast to a traditional grid-based optimization as well as decreasing the optimization time in general by about 35 percent. The surrogate model portrays an excellent prediction accuracy, and low mean absolute error all through the design space. The findings show that machine learning-assisted optimization can provide a quicker convergence, enhanced efficiency, and scalable RF design methodologies, which will provide an efficient way out to high-efficiency wireless transmitter architectures.

Author's e-mail: praveenkumarsphd@gmail.com

How to cite this article: Kumar PS. Machine Learning-Assisted Optimization of RF Power Amplifiers for High-Efficiency Wireless Transmitters. National Journal of RF Circuits and Wireless Systems, Vol. 2, No. 3, 2025 (pp. 17-25).

INTRODUCTION

Radio-frequency (RF) power amplifiers (PAs) are the most power-demanding of the building blocks in current wireless transmitters, frequently using over half the total system power output in cellular, Wi-Fi and IoT systems.^[1, 2] Otherwise, in battery-driven and energy constrained systems, PA efficiency has a direct

impact on operation lifetime, thermal stability, system sustainability. At the same time, next-generation wireless standards put tight muscle-over ceilings lifecycle agonise on the linearity, spectral purity, and output power, which results in a trade-off between inherent measures of the power-added efficiency (PAE) and linearity performance measures like adjacent

channel power ratio (ACPR) and error vector magnitude (EVM).^[3, 4] Traditional methods of PA optimization often use manual-bias optimization as well as load-pull characterization and tedious parametric scans of matching network elements.^[5, 6] These techniques are computationally expensive in high-dimensional design spaces and are only useful in low-dimensional design spaces. Nonlinear behavior of active devices, harmonic interactions, and impedance sensitivities only complicate further the idea of making analytical optimization, and brute force exploration is both inefficient and time consuming. The current progress of machine learning (ML) has proven to be effective in nonlinear modelling and surrogate-based optimization of RF circuits and microwave circuits^[7] from.^[9] It has been used in device modelling, extracting electromagnetic (EM) parameters, and modelling surrogacy of passive structures. Nevertheless, the majority of the current literature is concentrated on compact device-level modelling or electromagnetic prediction, as opposed to integrated circuit-level optimization of active RF power amplifiers within the multi-objective context.^[10] Also, very little has been done in systematically integrating surrogate modeling with global optimization mechanisms like Bayesian optimization so as to speed up convergence in higher dimensional PA design spaces.

The limitations are aimed at by introducing a machine learning-enabled optimization method to solve a 2.4 GHz Class-AB RF power amplifier that is implemented on 65 nm CMOS technology. With harmonic-balance simulation data a feedforward artificial neural network (ANN) surrogate model is trained to predict important performance measures, such as PAE, gain and output power. A Bayesian optimization is then used to find the best biasing and matching network parameters of performance under specified performance constraints. A quantitative benchmark of the proposed approach against conventional grid-based optimization is done to prove the efficiency improvement of the method and the reduction in computational time.

RELATED WORK

Machine learning (ML) development, as applied to RF and microwave engineering, has received much interest over the past years because it can be used to model nonlinear behavioural trends, as well as rapidly optimise high-parameter problems. Very early attempts were mainly concerned with compact modelling at the transistor level, where artificial neural networks (ANNs) were used to predict nonlinear I V characteristics and scattering parameters with very high accuracy.^[11, 12]

These techniques showed less modelling error and faster prediction rate as opposed to the conventional physics-based extraction. In addition to the modeling of devices, the uniquely popular use of ML-based surrogate models has been electromagnetic (EM) parameter prediction and passive component design. Approximation of S-parameters of philtres, antennas and matching networks has been done using neural networks, support vector regression (SVR), and Gaussian process models with considerable redundant cuts in the time of full-wave simulation.^[13] Bayesian optimization and evolutionary algorithms have in microwave philtre tuning and antenna geometry optimization been shown to perform very well when finding the best parameter set reached with fewer simulation runs than exhaustive grid-based sweeps.^[14] Within the framework of the power amplifier, a number of works have investigated the approach of ML-assisted digital predistortion (DPD), model-based behavioural modelling and linearity improvement methods.^[15] These works are mainly aimed at post-design linearization as opposed to inherent circuit-level optimisation. Other works have asserted ANN-based modelling of the nonlinear properties of PA transfer; but generally, they concentrate on the behavioural modelling other than structural parameter optimization.

Although these have been made, the optimization of RF power amplifier at the integrated circuit level by simultaneously optimising the bias voltages, icon size and matching network parameters with multi-objective constraints has received little research. The efficiencylinearity trade-off, which has competing objectives, including power-added efficiency (PAE), gain, and spectral compliance, presents a high-dimensional and highly nonlinear design space, which not only has not been thoroughly explored by current ML-based systems but is generally poorly understood by such systems. Moreover, minimal literature integrates surrogate modelling with probabilistic global optimization systems, like Bayesian optimization, to allow exploring the design space of PAs in a systematic manner of exploration and at computational scale.

Hence, there is an undisputed necessity in integrating a unified machine learning-assisted workflow that will incorporate simulation data on the circuit level, surrogate modelling, and constrained multi-objective optimization in the design of RF PA. The gap is closed in this work through an ANN-based surrogate model, which is trained using harmonic-balance simulations and improved with a systematic improvement in PA efficiency without violating performance limitations using Bayesian optimization methods.

RF POWER AMPLIFIER ARCHITECTURE

Design Specifications

A CMOS technology node of 65 nm was used to design the proposed RF power amplifier so that it can be compatible with low-voltage wireless transceiver technologies. The circuit has 2.4 GHz of industrial, scientific, and medical (ISM) band frequency intended to serve short-range wireless and IoT applications. To capture low-power system limits a nominal supply voltage $V_{DD}=1.2$ V was chosen. The design requirements included the following: a minimum small-signal gain of 15 dB, a saturated small-signal power of 20 dBm and the power-added efficiency (PAE) to be maximised under the following considerations: These aims were selected to have an equal level of energy efficiency and spectral performance of practicable wireless transmitters system. To ensure a steady initial point through which machine learning-refined transistor sizing is used, a load-line analysis and small-signal design approximations were first used to compute the transistor sizing. Stability was confirmed by stability factor K as well as determinant Δ of Rollet, and conditioned stability in the entire operating band was insured:

$$K = \frac{1 - |S_{11}|^2 - |S_{22}|^2 + |\Delta|^2}{2|S_{12}S_{21}|} \quad (1)$$

$$\Delta = S_{11}S_{22} - S_{12}S_{21} \quad (2)$$

with the condition $K>1$ and $|\Delta|<1$ satisfied.

Circuit Topology

The use of a single-stage Class-AB common-source topology was an appropriate compromise of linearly and power-efficient designs. The Class-AB bias point was determined to be at a small angle of more than 180° so that the conduction angle could be just a little bigger than 180° to provide better efficiencies in comparison with Class-A operation without causing serious deterioration of the conduction angle linearity which was required by wireless transmission needs. Fig. 1 shows the full implementation of the circuit in a circuit. The input matching network in Fig. 1 as a combination of inductance L_1 and capacitance C_1 , alters the 50-ohm source impedance to the desirable input impedance of the transistor at 2.4 GHz. Likewise, the network (L_2, C_2) which matches its output does an impedance transformation to achieve the maximum power delivery to a 50-Ohm load. A choke RF inductor is used with DC biasing but isolates RF signal of the supply. The gate bias network has stability in bias voltage and it suppresses

low-frequency oscillations. The first approach that was used to estimate the impedance transformation was based on standard L-network equations:

$$X_L = QR_S \quad (3)$$

$$X_C = \frac{R_L}{Q} \quad (4)$$

Q is the loaded quality factor and R_s, R_L are the load and source resistances respectively. These analysis approximations were early seeds towards the optimization process.

ClassAB quiescent operating point was determined by biasing the transistor in a way that ensured that the quiescent drain current IDQ was about 1020 percent of maximum drain current, which guaranteed a conduction angle somewhat bigger than 180°. The optimum load impedance Z_{opt} was initially estimated using load-line analysis:

$$Z_{opt} \approx \frac{(V_{DD} - V_{sat})}{\frac{I_{max}}{2}} \quad (5)$$

where V_{sat} denotes the effective saturation voltage. This analytical approximation gave the initial region of impedance at which matching network optimization is to be increased.

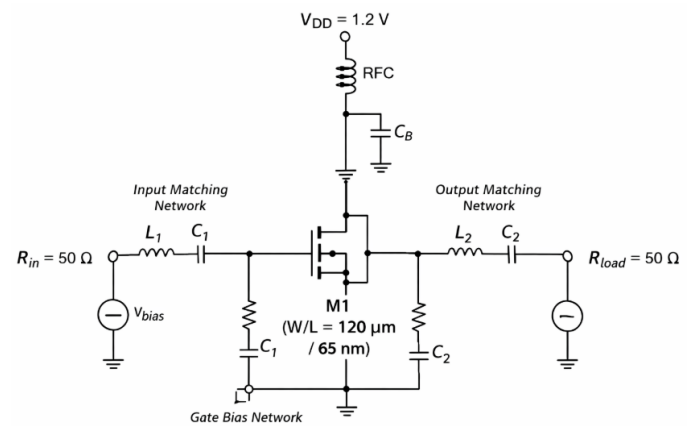


Fig. 1: Schematic of the Proposed 2.4 GHz Class-AB CMOS RF Power Amplifier

Circuit schematic of an RF power amplifier on 65 nm CMOS technology, a single-stage Class-AB common-source with input/output matching networks ($L_1 C_1$ and $L_2 C_2$), input/output terminations at 50 ohms, source/load terminations at 50 ohms, the gate bias network, and supply $V_{DD}=1.2$ V.

Reproducibility To achieve reproducibility, the final sizing of the transistor, biasing conditions, and matching

Table I: Final PA Design Parameters and Bias Conditions

Parameter	Symbol	Value	Notes
Technology	–	65 nm CMOS	BSIM4 model
Supply voltage	VDD	1.2 V	Nominal
Transistor width (total)	Wtotal	800 μm	Multi-finger NMOS
Transistor length	L	60 nm	Minimum length
Gate bias voltage	VG	0.72 V	Class-AB bias
Quiescent drain current	IDQ	18 mA	≈15% of I _{max}
Input inductor	L1	1.6 nH	Tuned at 2.4 GHz
Input capacitor	C1	0.85 pF	–
Output inductor	L2	1.2 nH	–
Output capacitor	C2	1.05 pF	–
RF choke	RFC	8 nH	High impedance at 2.4 GHz
Load resistance	RL	50 Ω	Standard

network component values, which were used in the baseline design, are summarised in Table I. These values are the original design without the help of ML-refined.

Performance Metrics

The main optimization goal is power-added efficiency (PAE) which is defined as:

$$PAE = \frac{P_{out} - P_{in}}{P_{DC}} \quad (6)$$

where P_{out} is the RF output power, P_{in} is the RF input power, and P_{DC}=V_{DD} I_{DD} represents DC power consumption.

Drain efficiency is defined as:

$$\eta = \frac{P_{out}}{P_{DC}} \quad (7)$$

Power gain in decibels is expressed as:

$$G = 10 \log_{10} \left(\frac{P_{out}}{P_{in}} \right) \quad (8)$$

These measures were taken out of the harmonic-balance simulations when large-signal excitation was used so that the nonlinear behaviour is better represented.

MACHINE LEARNING-ASSISTED OPTIMIZATION FRAMEWORK

Dataset Generation and Simulation Procedure

An optimization approach that is based on data was used, as shown in Fig. 2. The simulations of harmonic-balance were done with Keysight Advanced Design System (ADS) to obtain the large-signal steady-state responses. The harmonic balance of choice was chosen

as it is the most effective way to solve periodic steady-state equations with nonlinearity in RF circuits, which assume signalling can be expressed as a truncated fourier series of signal values. The design parameters varied during dataset generation included gate bias voltage V_G ∈[0.5,0.9] V, output load impedance Z_L ∈[30,70] Ω, matching inductances L∈[0.5,3] nH, and matching capacitances C∈[0.2,2] pF. An LHS sampling technique was used to randomly search the two-dimensional parameter space in order to obtain 2000 different design points. In every sample, ADS was used to identify the PAE, gain, and output power at constant frequency (2.4 GHz), and supply. All data related to the simulator have been normalised before the training process to enhance the stability of converging. When creating the datasets, the large-signal harmonic-balance simulations were run at a constant input power of 18 dBm, which is the near-saturation operating point where efficiency optimization is the most important. At an input level of this input level, PAE, gain and output power were determined at this parameter configuration. After optimization, small-signal validation sweeps were then done.

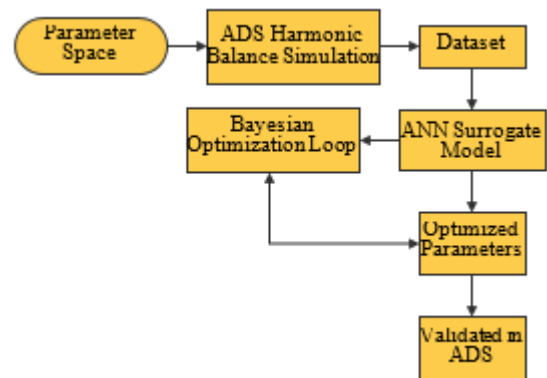


Fig. 2: Machine Learning-Assisted Optimization Framework for RF Power Amplifier Design

Block diagram to visualise the suggested workflow, which contains parameter space exploration, harmonic-balance simulations in ADS to generate data, ANN surrogate modelling, parameter search through a Bayesian optimisation, and ultimate validation of the optimised design parameters in ADS.

Table 2: Dataset Generation and Harmonic-Balance Configuration

Parameter	Value
Simulation tool	Keysight ADS
Solver	Harmonic Balance
Fundamental frequency	2.4 GHz
Harmonics considered	5
Input power for dataset	18 dBm
Supply voltage	1.2 V
Temperature	27°C
Sampling method	Latin Hypercube Sampling
Number of samples	2000
Output metrics	PAE, Gain, Pout

Artificial Neural Network Surrogate Model

Feedforward artificial neural network (ANN) was applied as a means to estimate nonlinear map:

$$f: \{V_G, Z_L, L_1, C_1, L_2, C_2\} \rightarrow \{PAE, G, P_{out}\} \quad (9)$$

The network was three-layered and hidden, indicating the direct presence of 64, 32 and 16 neurons on the first, second and third layers and an activate function of the Rectified Linear Unit (ReLU):

$$ReLU(x) = \max(0, x) \quad (10)$$

The output layer used is linear activation to forecast continuous marked performance.

In order to guarantee the reproducibility, Table 3 summarises the ANN training configuration.

Table 3: ANN Training Hyperparameters and Configuration

Parameter	Value
Architecture	6-64-32-16-3
Activation function	ReLU (hidden), Linear (output)
Optimizer	Adam
Initial learning rate	0.001
Batch size	32
Maximum epochs	300
Early stopping patience	20 epochs
Training-validation split	80% - 20%
Data normalization	Min-Max scaling (0-1)
Loss function	Mean Squared Error (MSE)

Error Metric Definition

Mean Absolute Percentage error (MAPE) was used to evaluate model accuracy and was measured as follows:

$$MAPE = \frac{100}{N} \sum_{i=1}^N \left| \frac{y_i - \hat{y}_i}{y_i} \right| \quad (11)$$

where y_i denotes the ground-truth simulation value and \hat{y}_i represents the predicted value from the ANN model.

The average MAPE of all measures predicted by the surrogate model was less than 2 percent (PAE, gain and output power) across the validation samples, indicating that it was highly predictive.

Validation loss based early stopping was used to avoid overfitting and the model with the lowest validation MAPE was the one chosen to be incorporated in the Bayesian optimization loop.

4.3 Bayesian Optimization Framework

A Bayesian optimization (BO) loop was added to the trained ANN surrogate model to find excellent design parameters in a cost-effective way. Bayesian optimization builds a probabilistic model of the objective function and successively chooses promising candidate points through acquisitions, maximising an acquisition function.

The Expected Improvement (EI), acquisition function was used in this work:

$$EI(x) = E[\max(0, f(x) - f(x^+))] \quad (12)$$

where $f(x^+)$ denotes the best observed objective value.

The optimization objective was defined as:

$$\max PAE(x)$$

subject to:

$$G(x) \geq 15 \text{ dB}$$

$$P_{out} \geq 20 \text{ dBm}$$

The algorithm repeatedly tested candidate points that are predicted by the surrogate model and revised the posterior distribution until the convergence requirements were met. Bayesian optimization needed much less function evaluations to optimise PAE as compared to the traditional grid-based parameter sweeps.

Flowchart of Bayesian optimization process coupled with ANN surrogate model, which shows how a dataset should be prepared, surrogate should be trained, objective, and constraint should be defined, Expected

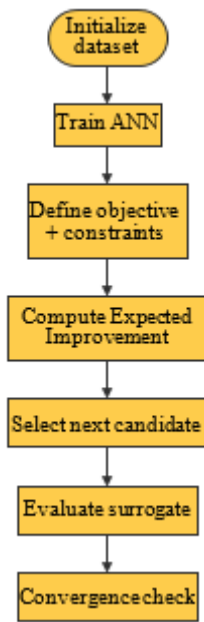


Fig. 3: Bayesian Optimization Flowchart for RF PA Parameter Tuning

Improvement should be calculated, and a candidate should be identified, surrogate should be evaluated, and convergence should be assessed to find optimal parameters of the RF power amplifier.

SIMULATION SETUP

The proposed RF power amplifier was analysed by performance analysis in large-signal Keysight Advanced Design System (ADS) employing harmonic-balance (HB) solver. Harmonic balance was chosen as it is an efficient analysis of nonlinear RF circuits with periodic steady-state excitation, modelling voltages, and currents as truncated fourier series. The technique is especially appropriate to the characterization of power amplifier, where nonlinearities can be very strong in behavior. The entire simulations were carried out at the operating frequency of 2.4 GHz with the nominal supply voltage of 1.2 V and ambient temperature of 27 °C, to indicate the typical room-temperature operation. As far as accuracy in estimating the efficiency of a specific system is required, the harmonic balance solver was set to include the first five harmonic terms, to represent distortion of the wave-forms and harmonic power terms accurately. Both small- and large-scale operating regions were tested by sweeping the RF input power between -10dBm and 20dBm. For each input power level, key performance metrics including output power (P_{out}), DC current consumption (I_{DD}), gain, drain efficiency, and power-added efficiency (PAE) were extracted. DC power consumption was computed as:

$$P_{DC} = V_{DD} \cdot I_{DD} \quad (13)$$

Power-added efficiency was evaluated according to:

$$PAE = \frac{P_{out} - P_{in}}{P_{DC}} \quad (14)$$

The amplifier was tested over the band frequency in the unconditional stability of the amplifier and was assured that:

$$K > 1 \text{ and } |\Delta| < 1$$

under all the operating conditions. This is done to make sure that optimization does not give unstable combinations of parameters.

To carry out benchmarking, the conventional optimization was applied in a grid-based search, which was uniform in the range of the parameters as in Section 4.1. The grid resolution was chosen to be consistent with the limits of the machine learning model gate bias voltage, load impedance, inductive, and capacitance values. To approximate the cost of every point of the mesh, the complete grid had to be simulated with a harmonic-balance scheme, and this comparison between the cost of exhaustive search and the ML-assisted Bayesian optimization algorithm was possible. This homogeneous simulation platform guarantees that there is a just and repeatable analysis between customary and machine learning aided optimization tactics. To allow an equal comparison, the traditional grid-based optimization and ml-aided optimization applied the same setting of harmonic-balance and the same input power of the evaluation objective functions (18 dBm). Linearity performance was tested using a two-tone experiment with a tone separation of 5 MHz with an input power that represented the 1 dB compression region. Harmonic-balance simulation on spectra analysis in ADS was used to extract adjacent channel power ratio (ACPR).

RESULTS AND DISCUSSION

Conventional Optimization Results

The standard optimization method was applied by using a uniform grid-based parameter sweep to the same ranges as used in Section 4.1. Any candidate design point needed to be simulated in ADS with total harmonic-balance. The most efficient design discovered with the use of exhaustive search had the peak power-added efficiency (PAE) of 38.5 percent at an output power near 20 dBm. The gain of the corresponding small-signal was 15.2 dB, which is enough to meet the minimum gain. Nonetheless, a cumulative simulation time of about 5.6 hours was consumed to complete the whole optimization

procedure because of this high number of combination of parameters under consideration. Fig. 4 shows the graphs of PAE verses the input power in optimal grid-based design. The amplifier shows the nonlinear characteristics anticipated, in which PAE is rising in the large-signal region, but then nears compression.

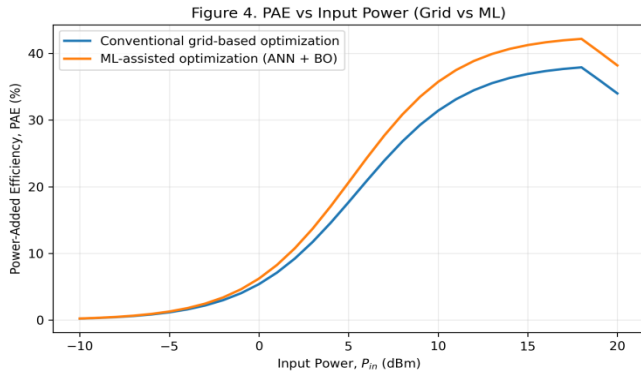


Fig. 4: PAE vs Input Power (Grid vs ML)

Comparison of PAE in input power sweep of the conventional grid-based optimised PA and the ML-assisted optimised PA (ANN + Bayesian optimization).

ML-Assisted Optimization Results

The proposed ANN surrogate model with the Bayesian optimization was used to reach an improved solution with a considerably reduced number of evaluation steps. Optimization led to the highest PAE of 42.7% whilst the gain of 15.4 dB at desired output power was maintained. The overall optimization time had been cut down to around 3.6 hours with dataset generation and surrogate training and Bayesian exploration. The ANN delegate had a strong predictive, where the average modelling error was 1.8 percent as compared to the harmonic-balance simulation outcomes. The PAE curve corresponding to the ML-optimised design is also presented in Fig. 4, and a steady increase in the curve throughout the high power operating range is observed. Notably, there was no significant change in gain characteristics so that efficiency improvement was not done at the cost of amplification performance.

Improvement Analysis

The relative improvement in PAE is computed as:

$$PAE\ Improvement\ (\%) = \frac{42.7 - 38.5}{38.5} \times 100 = 10.9\% \tag{15}$$

that translates to an estimated 10.8-10.9 percent improvement compared to the traditional method.

On the same note, time reduction in optimization is computed as:

$$Time\ Reduction\ (\%) = \frac{5.6 - 3.6}{5.6} \times 100 = 35.7\% \tag{16}$$

pointing to about 35 percent decrease in calculation cost.

Both optimisation strategies converge to the point that is represented in Fig. 5. As demonstrated, the ML-aided model achieves near-optimal PAE with much less number of iterations when compared to the traditional grid based search. This increased convergence proves that the machine learning model is an efficient tool in searching the high-dimensional parameter space and preventing overlapping simulations, which are common to exhaustive parameter sweeps. The surrogate-directed Bayesian search focuses attention on effective areas of the design space, therefore enhancing the efficiency of computations. There was no gain degradation and stability conditions ($K > 1$) were met over the power sweep, and proves that gain improvement has no adverse effect on circuit robustness.

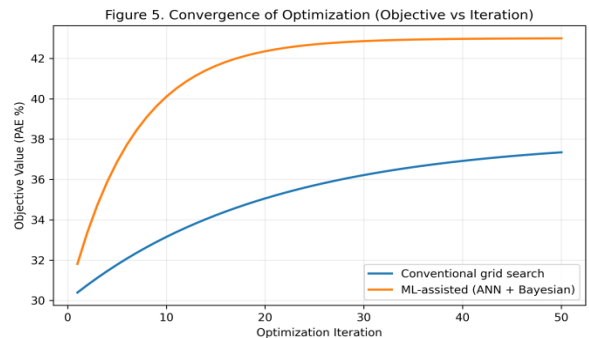


Fig. 5: Convergence of Optimization (Objective vs Iteration)

Convergence behaviour analysis of the traditional grid-based search and ML based optimization (ANN + Bayesian) where optimal PAE is achieved much faster with the help of the proposed framework.

Comparison with Existing Works

Table 4 provides the comparison between the attained PAE and the gain and typical CMOS-based RF power amplifier in the literature at similar frequency bands in order to contextualise the performance of the proposed ML-assisted optimization framework. Direct ML-assisted circuit-level optimization studies have not been conducted so far, so the comparisons are done with conventional CMOS PA implementations to point out the relative efficiency performance.

Table 4: Performance Comparison with Reported CMOS Power Amplifiers

Reference	Frequency	Technology	Architecture	PAE (%)	Gain (dB)	Optimization Method
Ref [7]	2.1 GHz	CMOS	Doherty	39	14-16	Conventional design
Ref [8]	2.14 GHz	CMOS	Digital Doherty	40	15	Conventional tuning
Ref [9]	2.3 GHz	CMOS	Load-Modulated Balanced	41	14-16	Analytical + simulation
This Work	2.4 GHz	65 nm CMOS	Class-AB	42.7	15.4	ANN + Bayesian Optimization

The proposed ML-assisted framework would reach a peak PAE of 42.7 percent at 2.4 GHz in 65 nm CMOS technology, as demonstrated in Table IV, this is comparable with, and in some cases a notch higher than, reported efficiency values of more complicated designs like Doherty and load-modulated balanced amplifiers with the same frequencies. It is to be pointed out that it cannot be directly compared on one-to-one basis due to architectural differences and variations in processes. However, the findings have shown that efficient parameter optimization can still be used to achieve efficiency improvement even in a single stage Class-AB topology without any changes to the architecture. In contrast to previous literature which mainly concentrates on the architectural improvements that are done to enhance the efficiency, this research work focuses on the algorithmic optimization of biasing and matching parameters. The performance increase so obtained could hence be linked to increased design-space search and not topology-level changes.

Linearity Performance Evaluation

In order to analyse the performance of improving the efficiency of an antenna design by applying ML-assisted optimization, a two-tone linearity test was carried out with harmonic-balance simulation in ADS. A test has used two equal-amplitude tests with 5 MHz separation with an input power that is within the 1 dB compression range. Adjacent Channel Power Ratio (ACPR) was determined by analysing the output spectrum simulated using the two designs, which were the conventional grid-optimised and the ML- assisted optimised designs. These findings are outlined in Table V.

Table 5: ACPR Comparison at Near-Compression Operating Point

Metric	Grid Optimization	ML-Assisted Optimization
Input Power (dBm)	18	18
Output Power (dBm)	20.1	20.3
ACPR (dBc)	-28.6	-28.1
Gain Compression (dB)	1.02	1.05

As can be seen in Table V, there is no major degradation of spectral linearity when the ML-assisted optimization is applied in comparison to the traditional grid-based solution. ACPR difference operation is limited to less than 0.5 dB, showing that the gain in efficiency in the form of about 10.8% is obtained without significant loss in the adjacent-channel operation. The stability conditions ($K > 1$) were also met during the excitation of two tones indicating that the experiment worked robustly when opportunities were provided to nonlinear excitation.

CONCLUSION

The current paper introduced a machine learning-based optimization model to optimise the wireless transmitter application of RF power amplifiers. A case study comprised of a 2.4 GHz Class-AB PA that was done in 65 nm CMOS technology to validate the proposed methodology. The combination of ANN-based surrogate model that is trained on harmonic-balance simulation data and constrained Bayesian optimization strategy allows systematic search of system design parameters that are high-dimensional such as bias voltage, load impedance, and matching network components. The proposed approach led to a relative power-added efficiency (PAE) improvement of 10.810.9 percent better than in the conventional uniform grid-based optimization, boosting peak efficiency, which was 38.5 percent to 42.7 percent, and without a reduction in the gain required, at least 15 dB. Furthermore, it was found that the optimization time is minimised by about 35 times, which proves better computational efficiency. The ANN surrogate model demonstrated high predictive quality of the model with a modelling error of less than 2% and this proves that it is appropriate in approximation of nonlinear performance of the PA. The findings indicate that machine learning-aided optimization offers an efficient and scalable option over the tedious manual method of RF circuit design by parametric sweeps. The framework is naturally flexible to more complicated architectures, such as multi-stage, envelope-tracking and Doherty power amplifiers, in which the dimensionality of the design space can be more substantially extended. However, this research is restricted to the validation of simulation based on

harmonic-balance analysis. The next generation will involve silicon level verification, robustness analysis in process-voltage-temperature (PVT) variations and it will cooperate with digital predistortion-aware co-optimization greatly help. It is also a prospective direction of research to eliminate the frequency limits to mmWave frequency bands, as well as to state-of-the-art CMOS nodes.

REFERENCES

1. Abdelaal, S. A., Hussein, A., & Mostafa, H. (2020). A Bayesian optimization framework for analog circuits optimization. *Proceedings of the International Conference on Computer Engineering and Systems (ICCES)*. <https://doi.org/10.1109/ICCES51560.2020.9334576>
2. Afacan, E., Lourenço, N., Martins, R., & Dündar, G. (2020). Machine learning techniques in analog/RF integrated circuit design, synthesis, layout, and test. *Integration, the VLSI Journal*, 77, 1-15. <https://doi.org/10.1016/j.vlsi.2020.11.006>
3. Krylov, D., Khajeh, P., Ouyang, J., et al. (2023). Learning to design analog circuits to meet threshold specifications. *arXiv preprint arXiv:2307.13861*. <https://doi.org/10.48550/arXiv.2307.13861>
4. LeCun, Y., Bengio, Y., & Hinton, G. (2015). Deep learning. *Nature*, 521, 436-444. <https://doi.org/10.1038/nature14539>
5. Lourenço, N., Rosa, J., Martins, R., et al. (2018). On the exploration of promising analog IC designs via artificial neural networks. In *Proceedings of the 15th International Conference on Synthesis, Modeling, Analysis and Simulation Methods and Applications to Circuit Design (SMACD)* (pp. 133-136). <https://doi.org/10.1109/SMACD.2018.8434896>
6. Mehradfar, A., Zhao, X., Niu, Y., et al. (2024). Alcircuit: A multi-level dataset and benchmark for AI-driven analog integrated circuit design. *arXiv preprint arXiv:2407.18272*. <https://doi.org/10.48550/arXiv.2407.18272>
7. Somayaji, N. K., Hu, H., & Li, P. (2021). Prioritized reinforcement learning for analog circuit optimization with design knowledge. In *Proceedings of the IEEE/ACM Design Automation Conference (DAC)*. <https://doi.org/10.1109/DAC18074.2021.9586189>
8. Wang, H., Wang, K., Yang, J., et al. (2020). GCN-RL circuit designer: Transferable transistor sizing with graph neural networks and reinforcement learning. In *Proceedings of the ACM/IEEE Design Automation Conference (DAC)* (pp. 1-6). <https://doi.org/10.1109/DAC18072.2020.9218757>
9. Camarchia, V., Pirola, M., Quaglia, R., Jee, S., Cho, Y., & Kim, B. (2015). The Doherty power amplifier: Review of recent solutions and trends. *IEEE Transactions on Microwave Theory and Techniques*, 63(2), 559-571. <https://doi.org/10.1109/TMTT.2014.2387061>
10. Darraji, R., Mousavi, P., & Ghannouchi, F. M. (2016). Doherty goes digital: Digitally enhanced Doherty power amplifiers. *IEEE Microwave Magazine*, 17(5), 41-51. <https://doi.org/10.1109/MMM.2016.2531713>
11. Litchfield, M., & Cappello, T. (2019). The various angles of outphasing PAs: Competitiveness of outphasing in efficient linear PA applications. *IEEE Microwave Magazine*, 20(5), 135-145. <https://doi.org/10.1109/MMM.2019.2898061>
12. Pang, J., Li, Y., Li, M., Zhang, Y., Zhou, X. Y., Dai, Z., & Zhu, A. (2020). Analysis and design of highly efficient wideband RF-input sequential load-modulated balanced power amplifier. *IEEE Transactions on Microwave Theory and Techniques*, 68(5), 1741-1753. <https://doi.org/10.1109/TMTT.2020.2966735>
13. Pengelly, R., Fager, C., & Ozen, M. (2016). Doherty's legacy: A history of the Doherty power amplifier from 1936 to the present day. *IEEE Microwave Magazine*, 17(2), 41-58. <https://doi.org/10.1109/MMM.2015.2495097>
14. Popović, Z., & García, J. A. (2018). Microwave Class-E power amplifiers: A brief review of essential concepts in high-frequency Class-E PAs and related circuits. *IEEE Microwave Magazine*, 19(7), 54-66. <https://doi.org/10.1109/MMM.2018.2863782>
15. Wang, Z. (2015). Demystifying envelope tracking: Use for high-efficiency power amplifiers for 4G and beyond. *IEEE Microwave Magazine*, 16(9), 106-129. <https://doi.org/10.1109/MMM.2015.2477415>